STUDY AND ANALYSIS OF THE CAVITATING AND NON-CAVITATING JETS PART ONE
Parameters Controlling Force, Power, and the Jet Behavior

by

Ezddin HUTLI[a,b,c*], Miloš S. NEDELJKOVIĆ[d], and Szabolcs CZIFRUS[a]

[a] Institute of Nuclear Techniques, Budapest University of Technology and Economics, Budapest, Hungary
[b] Department of Thermohydraulics, Centre for Energy Research, Hungarian Academy of Sciences, Budapest, Hungary
[c] Energy Engineering Department, Faculty of Mechanical Engineering, Budapest University of Technology and Economics, Budapest, Hungary
[d] Faculty of Mechanical Engineering, University of Belgrade, Belgrade, Serbia

Original scientific paper
https://doi.org/10.2298/TSCI190428333H

This paper presents the dependency of the jet power and the cavitation intensity on the working conditions of the cavitating and non-cavitating jet flow. This dependency is indicated by the cavitation erosion process and flow structure. The effects of working conditions on the cavitation erosion were experimentally investigated. The flow visualization was done using a high-speed photography recording system. The analysis shows that the erosion rate calculation and the visualization of the jet structure can be used as tools to estimate the jet strength, the jet actions, the jet power, and the performance of the jetting system.

Key words: *power, dynamic power, static power, kinetic energy, efficiency, erosion, cavitation intensity*

Introduction

Cavitation is counted as a common problem in the pumps, the valves, and the hydraulic systems – causing serious wear, crack, and failure which reduces the lifetime of that component. In addition, the cavitation causes distortion of the hydraulic performance, vibration, and noise. The study and analysis of the cavitation as a phenomenon and related parameters is a necessary step to prevent the cavitation or to decrease its strength and its side effects in the hydraulic systems or to utilize the cavitation as power phenomenon at industrial applications. Many methods exist to create the cavitation, one type of them is the cavitating jet generator. To expand the range of applications of the cavitating water jets (submerged in the water or in the air) and to improve their efficiency and quality, we need to precisely clarify the structure of the ultrahigh-speed cavitating water jet. The optimization of the working conditions such as geometrical and hydrodynamical conditions is an important process to intensively utilize the jet destructive power (cavitation destructive power). The cavitating water jets have been widely utilized for cleaning of complicated mechanical products, cutting of solid materials, and surface improvement of materials in various industry fields [1-4]. It has received much attention also in the environmental industry for the possibility of applications to the decomposition of toxic substances and purification of sewage [5-9]. For efficient design and performance prediction of high-speed liquid jet

* Corresponding author, e-mail: ezddinhutli@yahoo.com

(cavitating and non-cavitating) generators, much attention has been directed to use the experimental investigation and numerical simulation in this field [10-15]. To determine the optimum working conditions and to measure the potential capability of such a system, the most effective system parameters should be specified. In the case of the cavitating water jet for cavitation erosion testing, the most effective parameters are the jet pressure (injection pressure), jet speed (exit jet velocity), cavitation number, dimensionless distance (x/d) and the nozzle geometry [16, 17]. To determine the most effective parameters of a water cavitating jet for testing materials resistance, two dependent variables were considered: the erosion depth and the specific energy [Jg^{-1}] needed to create the erosion process. For this purpose, the evaluation of the specific energy of the jet after exiting the nozzle is important, rather than the input energy to the system (pump power) [18]. However, the use of the concept of input energy makes it difficult to consider the real impact energy of a cavitating jet, as well as the dependence of energy on standoff distance. Thus, an alternative energy concept is needed to estimate erosion depth (cutting depth) properly [16, 17, 19]. The submerged cavitating jet is created by injecting the fluid through a nozzle with a certain power in a chamber filled with liquid; here the source of this power is the feed pump. At any point in the jet trajectory, the part of the jet in that point has a certain power. This power has three components of the power; the potential power (it is a function of elevation), the static power (it is a function of the pressure difference), and the dynamic power (it is a function mainly of the jet velocity). For the whole jet, the jet dynamic power *kinetic energy* is divided into two parts, one part is for driving the jet to its end point (*i. e*. net kinetic energy of the jet) and the other part is dissipated during interaction between the jet and the surrounded fluid in the form of shear process and formation of vortices and as a consequence the cavitation is a result [20]. Generally, according to the concept of conversion efficiency, it was found that, in cavitating systems, the input power which is transferred to the liquid is less than that consumed by a particular device. As an example in the case of the ultrasonic cavitating system, about 15% of the total power was utilized, while for the cavitating jet it was about 60-80% of the input power. In addition, the water jet-induced cavitation can achieve oxidation as an example to oxidize organic compounds pnitrophenol (PNP) with up to two orders of magnitude greater energy efficiency of ultrasonic [21, 22]. Even the power consumption by cavitation generators and improvements of their efficiency is an interesting subject for investigation but there is a dearth of studies on this subject. This study attempts to contribute to this topic. This paper focuses on the importance of the jet dynamic power as a parameter to measure the performance of the cavitating and non-cavitating jet; the different forms of the jet power are discussed, and the cavitation intensity was investigated based on the jet dynamic power and other parameters. In this paper, high-speed photography as a non-destructive method is used to detect, diagnose, and analyze the cavitation phenomenon. A high speed submerged cavitating jet generator was used as a tool for creating the cavitation as cavity clouds. The visualization data were processed to study the cavitation clouds behavior, structure and to measure parameters which are used to characterize the clouds. The obtained results were carefully analyzed. It has been found that the structure of cavitation clouds can be used successfully as an indicator of the influences of the applied working conditions on cavitating jets characteristics, application, performance, and quality.

Cavitating jet facility and measurements procedures

Figure 1 illustrates schematic diagrams of the cavitating jet generator, the test section (test chamber), the nozzle (a mounting way for the divergent and convergent case), and position of energy calculation points. The test chamber volume is 0.87 L with maximum pressure reaching 10 bar. A group of nozzles was used for measurements. The used nozzles are constructed of

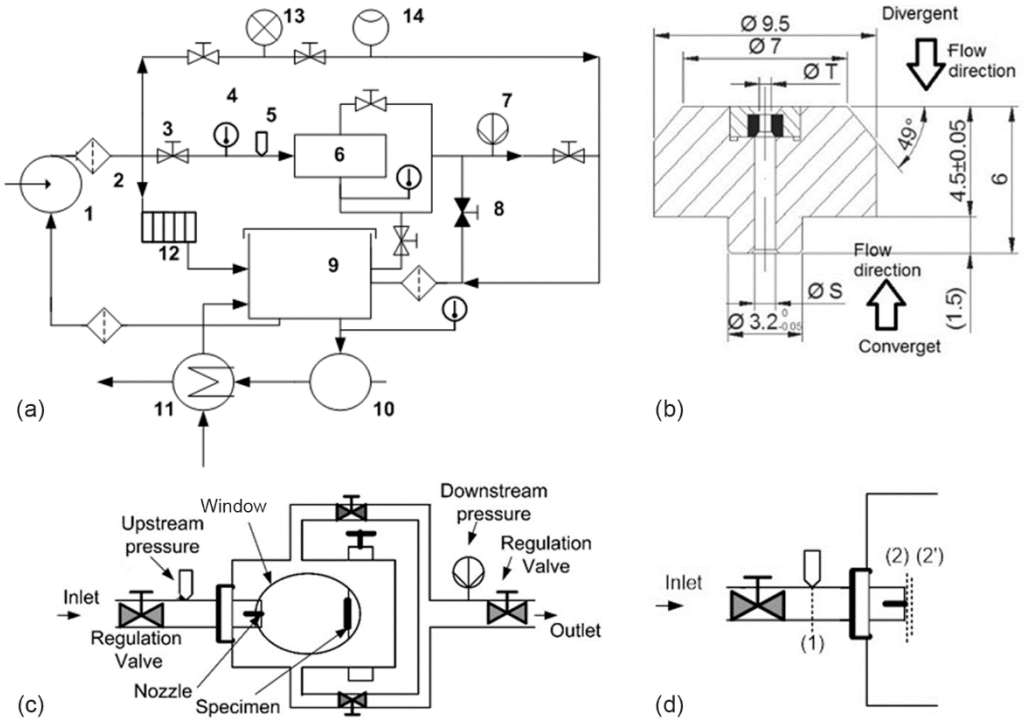

Figure 1. (a) Schematic diagram of the cavitating jet generator; *1 – plunger pump, 2 – filter, 3 – regulation valve, 4 – temperature sensor, 5 – high pressure transducer, 6 – test chamber, 7 – low pressure transducer, 8 – safety valve, 9 – tank, 10 – circulation pump,11 – heat exchanger, 12 – distracter energy, 13 – pressure gauge, 14 – flow indicator*, **(b) nozzle geometry [mm], two rows show possible ways of mounting in the test chamber, (c) a schematic diagram of the test chamber, (d) part of the test section showing the position of energy calculation points**

the stainless steel nozzle body and a sapphire orifice, their special design contributes to high stability and reliability. These nozzles are originally intended for water-jet cutting. Three transparent windows were provided, two at both sides and third at the top of the chamber. Thus, the cavitating jet can be observed and photographed. The test water was pressurized by a plunger pump and injected through the test nozzle into a water-filled test chamber, where the erosion specimen was mounted to be coaxial with the nozzle. with appropriate hydrodynamic and geometrical conditions, the cavitation is created. Figure 2 shows the appearance of the cavitating jet at different working conditions, these visualization results of cavitating water jet issuing from an orifice nozzle are presented and its applicability to intensively cavitating jets is demonstrated. The FASTCAM-APX high-speed video camera system was used for the visualization. For pressure regulation in the cavitating jet system, the system was provided with a group of valves and pressure gauges. The working fluid temperature is maintained within the maximum of 1 °C of variation during the tests. The temperature control is achieved using a cooling circuit consisting of a circulating pump, the heat exchanger, temperature sensors and temperature regulator device.

The injection pressure, *the upstream pressure of the nozzle*, P_1, was controlled manually by adjusting the rotational speed of a plunger pump. The downstream pressure of the nozzle, P_2, was controlled manually by adjusting the downstream valves. The main parameter to

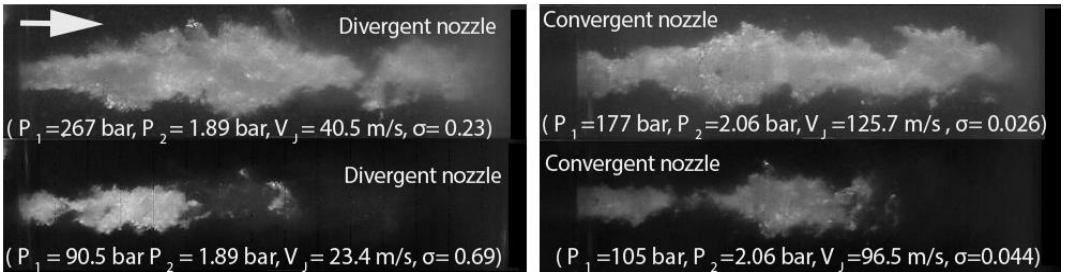

Figure 2. Photographs of the appearance of the high submerged cavitating jet at different hydrodynamic and geometrical conditions. Adapted from [23]

measure the cavitation created by cavitating jet is the cavitation number, σ, which is defined by the upstream pressure, P_1, the downstream pressure, the vapor pressure of the test liquid, exit jet velocity, V_J, and working fluid density, ρ. To discuss the effect of the nozzle geometry at a different value of jet power, P_{jet}, the exit jet velocity, V_J, is needed for both, the cavitation number, and the jet dynamic power calculation. For that, the discharge coefficient of each used nozzle was determined by measuring the flow rate for each nozzle at different jet power (different injection pressure) during the calibration process of the test rig equipment.

Calibration and uncertainties

In order to get a highly accurate result, the calibration is performed for all apparatus in the jet generator facility. First, the temperature sensors were calibrated in the circuits by measuring the known temperature of the water. The calibration was done with the help of digital thermometer named NORMA (maximum temperature is 400 °C with error 0.1 °C) which was used as a reference in the calibration process. Second, we examined the cooling system in the jet generator. This examination started by establishing the status of the heat exchanger and it is functioning. Here we tried to fix the maximum interval range of increasing the temperature around 4 °C in the test chamber over the desired working temperature. In this range the vapor pressure, $P_v(T)$, and the fluid density, $\rho(T)$, do not change appreciably by that we are avoiding the change in cavitation phenomenon. The static calibration of pressure transducers was performed using a standard dead-weight calibrating pressure tester. A reference pressure transducer used was HUBER. The output signals from the transducers (ED 210 and PE100) after converting these signals to a digit equivalent numbers [V] through the DMC 9012 were plotted versus the measured pressure with HUBER reference pressure transducer. This step was used to find the relationship between the output signals and the applied pressure. By curve fitting and finding the constants in the line equation were found. To assess the reproducibility and error reduction, ten reading outputs were used in each step. The average of the ten reading pressures was used in subsequent considerations. All calculations and measurements were made with LAB-VIEW which is used for acquiring the data and to drive the DMC 912 analog to digital converter. From the results, we can note that the two transducers are working at different error levels. The high-pressure transducer (ED210 HANNI) has an error of about 20 mbar. The low-pressure transducer (PE100 GMBH) has an error about 8mbar. The upstream pressure, P_1, and downstream pressure, P_2, were measured at the inlet and outlet of the test chamber, respectively.

Influence of nozzle geometry on the jet's power and cavitation characteristics

To declare the influence of the nozzle geometry on the jet dynamic power, P_{dyn}, a group of divergent and convergent nozzles with different dimensions were tested under different values of jetting power, P, and the characteristics of obtained cavitating jets were investigated.

The jet power was varied via the upstream and downstream pressures (P_1 and P_2), respectively. The valves at the inlet and outlet of the test chamber were used to adjust these pressures, fig. 1. The working fluid temperature was kept constant during the investigation.

The super-cavitating flow regime was chosen as a working region as in fig. 8. In order to simplify the idea and to describe well the power of the jet and the energy of the fluid, we have assumed that the flow is one phase thus averaged exit velocity, V_J, was computed from the flow rate, Q. Generally, depending on the inner geometry of the nozzle, at a low injection pressure, the cavitation might get started and get collapsed somewhere inside the nozzle, this stage of cavitation is classified as an inception stage [23, 24]. Because of the impossibility to visualize the flow inside the nozzle itself, the cavitation inside the nozzle is out of the scope of this work. As the injection pressure, P_1, is increased, the flow regime changes to a developing cavitation stage, where the cavitation appears at the outlet of the nozzle as a coherent structure finally reaching the super-cavitation stage. In this stage, the cavitation mixture is long enough to cover a big part or whole jet trajectory. The cavitation phase at the outlet of the nozzle decreases the flow area, resulting in a decrease of the discharge coefficient. In this work, only on the super-cavitation stage has been analyzed, which was characterized by appearing the cavitation at the outlet of the nozzle. It was found that the characteristic length and thickness of the super-cavitation mainly depends on upstream and downstream pressure, cavitation number, nozzle geometry and also the stand-off distance. The super-cavitating stage prevents the liquid jet from the intensive friction with the surrounding therefore there is less of momentum change with surrounding [25].

The super-cavitation patterns created using cavitating jet generators as applied in this work are not in contradiction to that one established by cavitation tunnel on the hydrofoil, or by cavitating propellers used in submarines, torpedoes, and other hydraulic machines. The principle of both is the same (decreasing cavitation number), while the functions are not. In the hydraulic machines, which use a special geometry design shape of the object to create the cavitation regime, the super-cavitation envelopes the object itself, which results in a great decrease of the skin friction drag on the object, thus enabling high speeds. Therefore, in hydraulics machines, the super-cavitation is the stage where cavity length exceeds the characteristic length of the body *object*. The cavitation bubbles are controlled to have desirable characteristics and not to collapse on the body. In the case of cavitating jet, the super-cavitation is used to increase the cavitation intensity, thus the severity of the cavitating jet will be enhanced. The super-cavitation in the cavitating jets is created in such a way that bubbles collapse on the target specimens placed in front of the jet, resulting in high erosion of the material (the intensity and aggressiveness increase as we move from one stage of cavitation to another) [3, 4, 16, 17].

The reason for choosing these working regimes is to achieve measurable cavitation damage. The cavitation has a shape of the cone around the liquid jet and the reducing of the friction drag allows for the achievement of very high jet speed, so the jet stagnation pressure is higher as proved by Momma and Lichtarowicz [26]. Therefore, as the cavitation number is decreased, the momentum and energy exchange along the jet trajectory decrease. Back to the

topic of the jet power, the total power at any point is composed of three types of power (static, potential and dynamic power) as in eq. (1). Where the Bernoulli equation (energy shape) is multiplied by the flow rate to have power shape. The dynamic power $P_{dyn} = 0.5\rho V_J^2 Q$ is the effective part of the total power, as it creates and drives the cavitating jet (cavitation clouds). Figures 3-7 present the relation between the jet dynamic power, the flow rate, Q, and the upstream pressure, P_1, the *injection pressure*. The potential power is considered as a constant value (no change in elevation), while the static power has effects on the intensity of the cavitating jet because the cavitation number, σ, is equal to a ratio of the static and dynamic power as shown later. The values of cavitation number are depending on a formula which is using for calculating the cavitation number as presented in fig. 8. The energy and power equations among the three points as in fig. 1(b). or any other arbitrary points along the jet trajectory can be written based on the Bernoulli equation, eq. (1), the flow rate, Q, was introduced to have power instead of energy. In this analysis, the first assumption is that the cavitation starts at the nozzle exit, as in fig. 2. The second assumption is the infinitesimal distance between the other two points (2 and 2') *i. e.* the point 2' is exactly at the nozzle exit. At the point 2', the pressure of the flowing liquid and the fluid around will suddenly decrease to the value between the pressure of the test chamber and the saturation pressure of the working temperature (vapor pressure). This sudden decrease in the pressure will liberate the gas bubble (non-condensable gas) which speeds up the creation process of the phase change that will exist as a result of the shear force and the vortex movement. The shear stress between the flowing fluid (jet) and the stationary liquid in the test chamber increases as a result of an increase in the jet dynamic power. The vortices with high circulation movement are created at the liquid jet periphery. The bubble is created because of the reduction of the pressure in the center of each vortex. Because of the circular shape of the entrance jet the bubbles, which were created around the jet (the jet is bounded by cavities), will be contacted among each other and cavity clouds will be formed as a result. By the way, for getting a spate of cavity rings, a pulsed jet is needed. The vortices strength is mainly dependent on the dynamic power of the jet. Thus the increasing of the jet dynamic power enhances the evaporation process at a constant temperature. This process as mentioned earlier is a result of the shearing process between fluids having a big difference in their kinetic energies:

$$\frac{P_1}{\rho}Q + 0.5V_1^2 Q + gz_1 Q = \frac{P_2}{\rho}Q + 0.5V_2^2 Q + gz_2 Q + \text{loss} = \frac{P_{2'}}{\rho}Q + 0.5V_{2'}^2 Q + gz_{2'} Q + \text{loss} \quad (1)$$

The jetting pressure (injection pressure) is highly correlated with the jet generation power mainly the jet dynamic power. High injection pressure drives an increase in exit-jet velocity. This aspect indicates that higher injection pressure generates greater power of the jet. Figures 3-7 clearly show that an increase in the power of the jet has a non-linear relationship with increasing water pressure (injection pressure); this may be depicted by a concave curve as shown in case of static power, fig. 3(b), while for the dynamic power, figs. 3(a), and 4(a), because the obtained curves overlap each other (they were nearly equal) the log scale was used thus the straight lines are obtained. In addition, injection pressure also affects the water flow rate. High water pressure generates a greater water flow rate at a given nozzle diameter size. A comparison of the power between the divergent and convergent curves shows the effect of the water flow rate according to the control of the injection pressure.

In figs. 3 and 4 the power curves (generated energy as a function of water pressure) is plotted for different nozzle geometry and dimensions (convergent and divergent shape). Meanwhile, each curve is calculated for a constant nozzle shape and diameter, the changing of injection

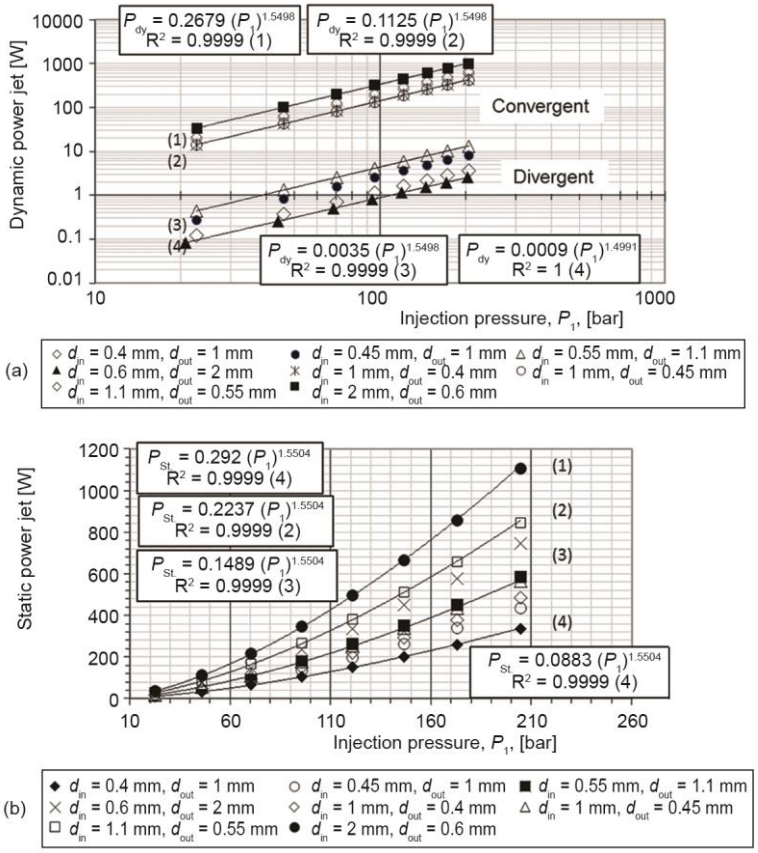

Figure 3. Effects of injection pressure on (a) jet dynamic power, P_{dyn}, (b) jet static power, P_{stat} (cavitating flow-cavitating jet)

pressure is achieved by changing the pressure from the pump. The divergent nozzles display lower energy than the convergent nozzles at a certain injection pressure level because the exit jet velocities are not equal. The difference in the amount of power, between the conditions indicated by curves, is increased with increasing pressure (injection pressure). These phenomena indicate that injection pressure affects the power level directly in terms of the exit jet velocity, and indirectly in terms of the vapor/liquid volume ratio (void fraction) consequently the terms of shedding/discharging frequency and collapsing energy thus the system performance will be affected [16, 17, 23]. The analysis also reveals that both the nozzle geometry and dimensions have a big influence on the jet dynamic power when the other parameters are kept constant. In addition, during the investigation of the effect of injection pressure on the dynamic power, it was found that the dynamic power is more sensitive to the variation of the nozzle geometry and/or outlet nozzle diameter than to that of the injection pressure and used pumped power. This suggests that extra energy can be generated by accelerating the fluid, because of the reduction in the flow area (which may be counted as the *saving power*). The dependency of the jet dynamic power on nozzle geometry and diameter shown in figs. 3(a) and 4(a). Figures 3(a) and 4(a) show a gap between the curves obtained by divergent and that who obtained by convergent nozzles.

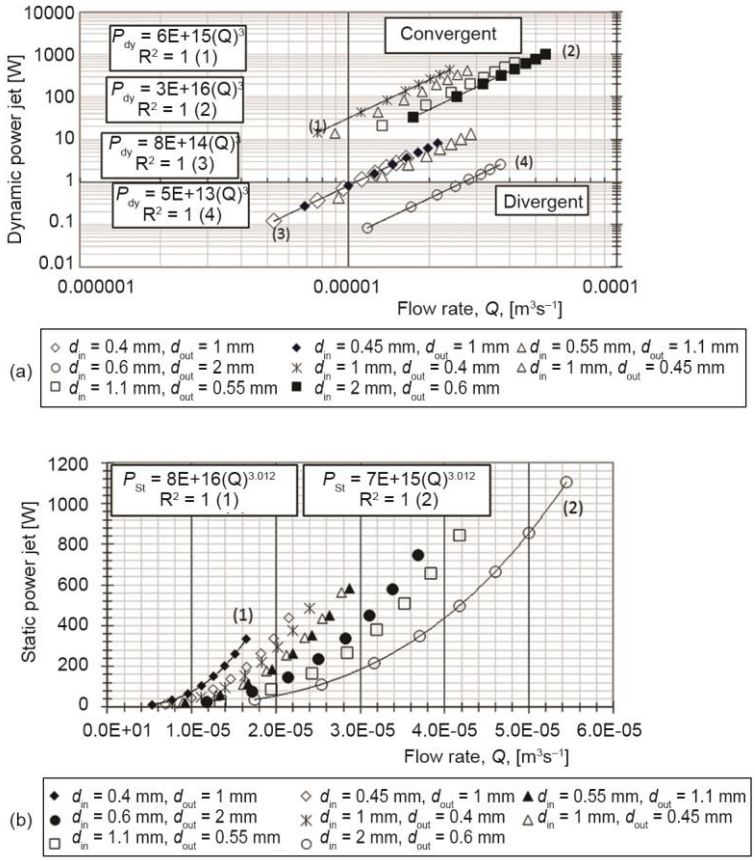

Figure 4. Influence of flow rate, *Q*, on jet dynamic power, P_{dyn}, (b) jet static power, P_{stat} (cavitating flow-cavitating jet)

Related to the static power, the analysis of figs. 3(b) and 4(b) reveals that, both the nozzle geometry and nozzle dimensions did not show a clear effect on the static power (loss) and there is no gap between the divergent and convergent nozzle results. In addition, fig. 3 shows that the injection pressure as the tested parameter has a significant influence on both kinds of power (dynamic and static). Based on the results shown in figs. 3(a), 3(b), and 4(a), 4(b), the relation between the different types of power (static power, *power loss* and *dynamic power*) and the injection pressure, P_1, and flow rate, Q, can be expressed mathematically as a power function relationship (the constants in the relations depend on the kind of power). Since we are interested in dynamic power we present here, for example, the relations between dynamic power and injection pressure and flow rate are, $P_{dyn} = A_1 P_1^{N_1}$ and $P_{dyn} = B_1 Q^{N_2}$, respectively, where the constants A and B depend on the nozzle geometry (shape and dimensions) and N_1 and N_2 depend on the tested parameters P_1 or Q. Figures 5-7 confirmed these relationships for a wide range of injection pressure and for a wide range of nozzle diameters. In the relationships, $P_{dyn} = A_2 P_1^{N_3}$ and $P_{dyn} = B_2 Q^{N_4}$, from the figures, it can be noted that $B_x \gg A_x$.

Figure 2 shows that the geometry of nozzles plays a significant role in the hydrodynamic behavior of the cavitating water jet. It means that the nozzle geometry plays a role in the jet power and its dissipation. This can be deduced from the jet penetration length and its thick-

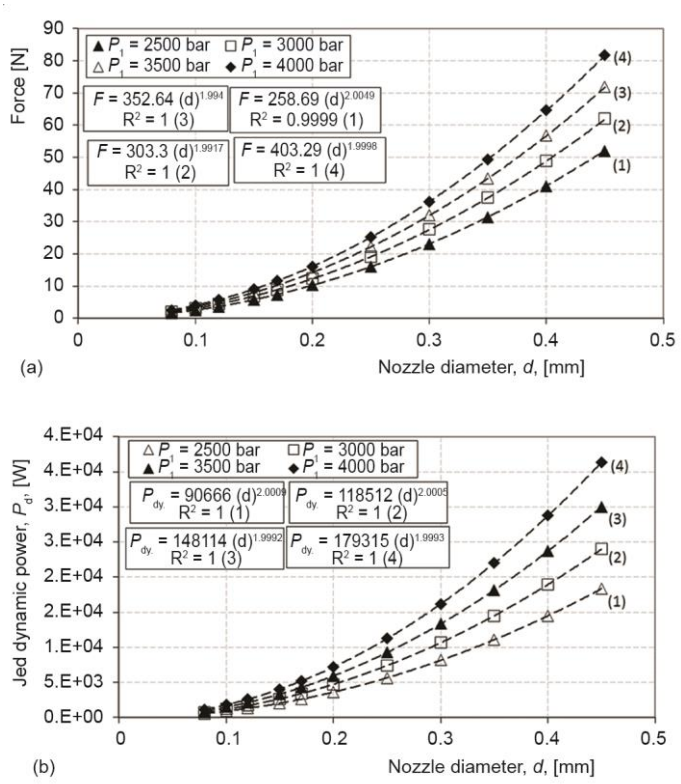

Figure 5. Influence of nozzle diameter, d_{out}, on (a) water jet force, F_J, (b) water jet dynamic power, P_{dyn}, (non-cavitating flow-liquid jet). Adapted from [26]

ess, as it will be shown later. As the total power (injection pressure) increases, the dynamic power will increase, the shedding and discharging frequencies of the cavitation cloud (bubble) are increased [23, 27-30]. Depending on the working power *injection pressure*, the cavitating water jets maintain their kinetic energy for a certain distance downstream of the nozzle, resulting in dimensions, shape, and strength of cavitation clouds.

At low working power, cavitating jets break up into fragments soon after leaving the nozzle. These fragments take the form like hairs or wires or individual bubbles; a cloud of very fine bubbles is formed characterized by low kinetic energy. Such bubbles will not create any damage in the target surface: diminished cavitating jets far from the target surface have practically no power and are therefore unable to attack the target, see fig. 2 (low injection pressure), and fig. 9. Figures 5-8 illustrate the influence of the geometry and working power for the non-cavitating jet (one-phase flow), where the difference between the applied pressures (power) in cavitating and non-cavitating water jets can be deduced from figs. 3-8. The represented data of non-cavitating jet have been obtained from the International Active Swiss Company (Mvt-Micro Technologies) [26]. There are many factors influencing cavitating jet breakup process among them the flow properties, interactions between the jet and the ambient fluid, and nozzle internal flow conditions. The studies by Hiroyasu [31], showed that, in nozzle geometries that favor cavitation, the main cause of the water-jet breakup is the cavitation onset within the nozzle

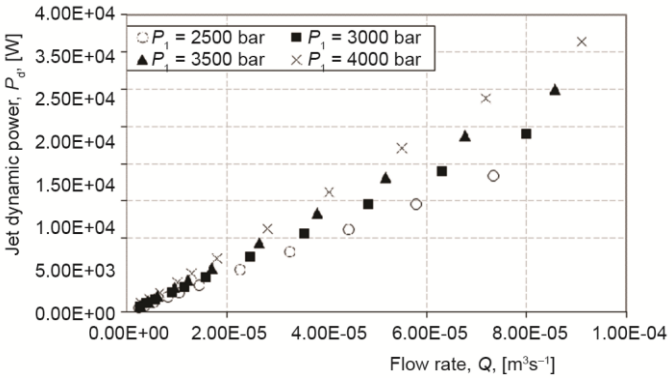

Figure 6. Jet dynamic power with the injection pressure, P_1 (non-cavitating flow-liquid jet). Adapted from [26]

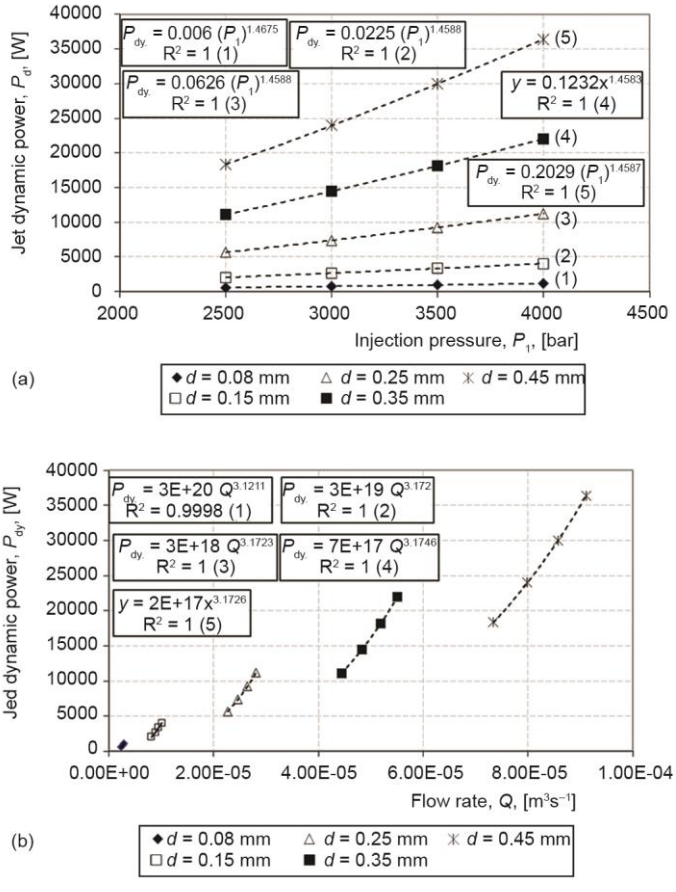

Figure 7. Jet dynamic power with (a) nozzle diameter, d_{out}, and injection pressure, P_1, (b) nozzle diameter, d_{out}, and flow rate, Q (non-cavitating flow-liquid jet). Adapted from [26]

which lead the strong disturbances that appear in the flow. This is usually the cause of the break up for non-cavitating jets too [30-34]. As found in previous works, the nozzle cavitation depends strongly, among other things, on nozzle shape, length, inlet and outlet diameter, surface roughness, and taper angle. In case of super-cavitation, the breakup is a result of many factors such as collapsing of the vapor bubbles in the jet, the distribution of the pressure, velocity and the density of jet components, liquid and bubbles (vapor and gases), and the forces exerted by surrounding on the jet [23, 27, 28]. Generally, for getting a well jetting process, it is obligatory to have an optimization situation between the desired flow rate and the available jet dynamic power. The flow and dynamic power are functions of the nozzle geometry and the injection pressure (injection power). There is a certain nozzle geometry (including the inlet and outlet diameters, length of the nozzle, roughness, angle of taper, *etc*.) that can be optimized to the pump specifications to maximize utilization of all the available energy. In the simple case when

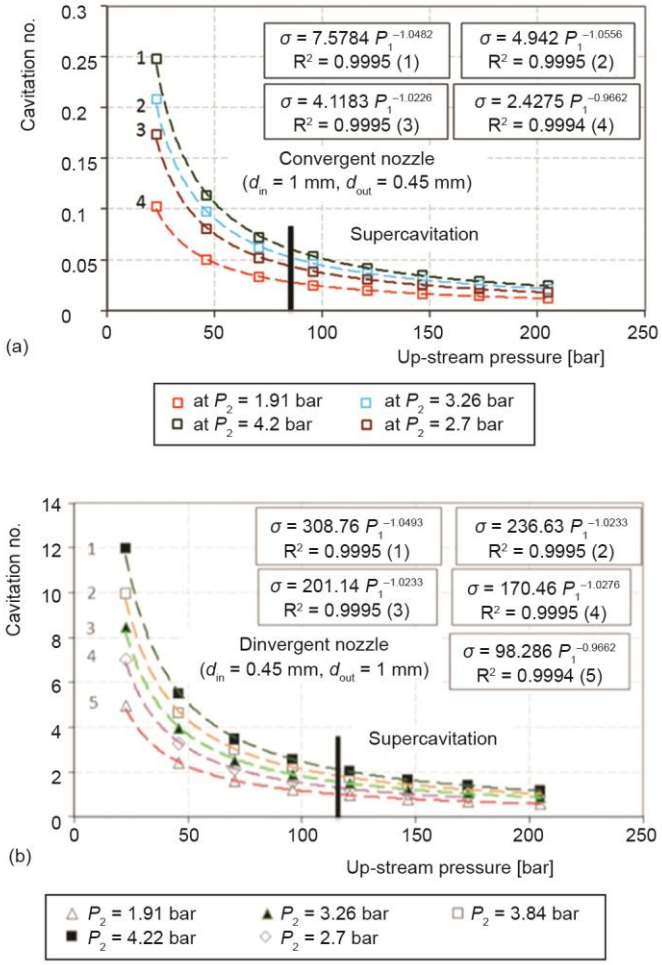

Figure 8. Determination of the working region based on the cavitation number and upstream pressure curve; (a) convergent nozzle, (b) divergent nozzle

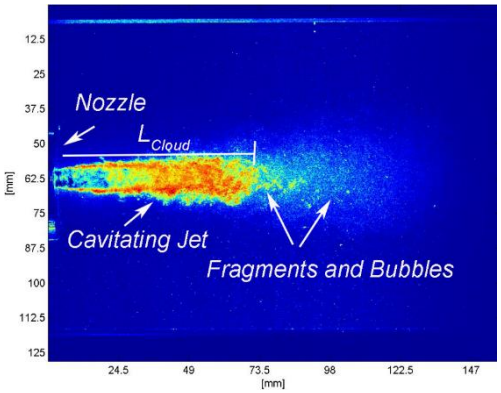

Figure 9. Photograph shows the cavitating jet life stages along its trajectory (cylindrical nozzle-diameter d = 7 mm, L_{Nozzle} = 20 mm, P_1 = 50 bar, P_2 = 2.3 bar, T = 21 °C)

the nozzle area is small, the system backpressure limits the full use of the available energy. Likewise, if the total nozzle area is increased, the jet velocity is reduced. In the case of cavitating jets, the maximum benefit from the available injection power can be achieved by optimizing the nozzle geometry for the highest dynamic power which leads to the highest cavitation intensity. Since jet action (*e. g.* erosion) depends mainly on the dimensionless stand-off distance (x/d). As shown in fig. 10, the nozzle geometry associated with stand-off distance is the key determinant of the performance of a jet and its behavior in time and space [10, 12, 13].

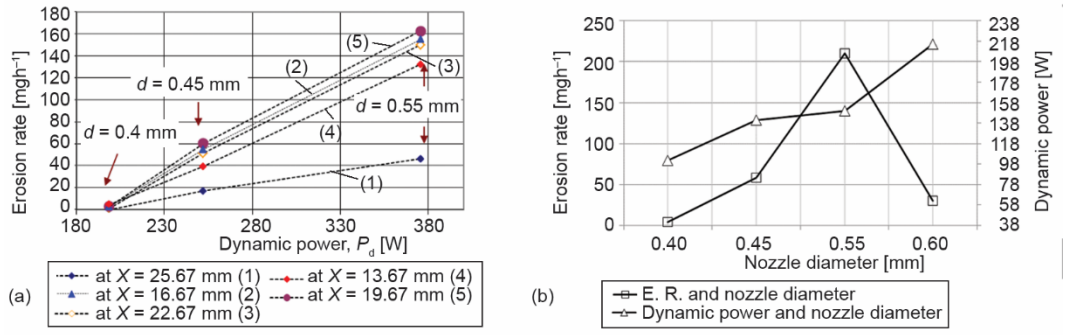

Figure 10. The cavitation erosion rate of pure copper (Cu) with (a) stand-off distance and nozzle diameter at constant dynamic power conditions in tab. 1, (b) nozzle diameter at different dynamic power conditions in tab. 2

Table 1. Hydrodynamic conditions for the x/d_{out} investigations with 1800 seconds exposure time

d_{out} [mm]	P_1 [MPa] ±0.1	P_2 [MPa] ±0.1	V_J [ms^{-1}] ±0.5	σ [–] ±0.001	T [°C] ±1
0.40	12.36	0.309	101.1	0.040	19
0.45	12.1	0.31	101.4	0.040	19
0.55	14.54	0.31	101.3	0.040	19

Table 2. Test conditions for the investigation of varying nozzle diameters with 1800 seconds exposure time

d_{out} [mm]	P_1 [MPa] ±0.1	P_2 [MPa] ±0.01	Q [m^{3}s^{-1}] ±0.1	V_J [ms^{-1}] ±0.5	σ [–] ±0.001
0.60	16.534	0.420	3.25E-05	115.0	0.048
0.55	16.534	0.368	2.57E-05	108.0	0.045
0.45	16.534	0.320	1.92E-05	121.0	0.029
0.40	16.534	0.308	1.47E-05	117.3	0.030

Conclusion

The result of the analysis associated with the experimental work which was carried out to enhance the performance of the cavitating and non-cavitating jet declare the relevant parameters controlling the jet behavior, its force and its power. The obtained results support the presented analytically derived formulas, which can be used to predict and estimate the jet action for various conditions. The effect of nozzle geometry dominated over all other parameters of jet performance and quality.

Acknowledgment

The authors would like to express their thanks to Prof. Gergely Kristof at Department of Fluid Mechanics and Prof. David Legrady at NTI-BME for their valuable comments for the first author during the writing of the paper. First author is also grateful for the Ministry of Science in Libya for support during his research activity. Libyan government paid to EPFL-LHM for using some equipment. The authors would like to express their thanks to the International Active Swiss Company (mvt AG) for the permission to use their data in this paper.

References

[1] Soyama, H., Improvement of Fatigue Strength by Using Cavitating Jets in Air and Waste, *Journal of Materials Science, 42* (2007), 16, pp. 6638-6641
[2] Hutli, E., *et al.*, Plastic Deformation and Modification of Surface Characteristics in Nano-and Micro-Levels and Enhancement of Electric Field of FCC Materials Using Cavitation Phenomenon, *Mechanics of Materials, 92* (2016), Jan., pp. 289-298
[3] Hutli, E., *et al*., The Ability of Using the Cavitation Phenomenon as a Tool to Modify the Surface Characteristics in Micro and in Nano Level, *Tribology International, 101* (2016), Sept., pp. 88-97
[4] Hutli, E. *et al.*, Controlled Modification of the Surface Morphology and Roughness of Stainless Steel 316 by a High Speed Submerged Cavitating Water Jet, *Applied Surface Science, 458* (2018), Nov., pp. 239-304
[5] Dular, M., *et al.*, Use of Hydrodynamic Cavitation in (Waste) Water Treatment, *Ultrasonics Sonochemistry, 29* (2016), Mar., pp. 577-588
[6] Dindar, E., An Overview of the Application of Hydrodynamic Cavitation for the Intensification of Wastewater Treatment Applications: A Review, *Innovative Energy & Research, 5* (2016), 1, pp. 137-144
[7] Yunfeng, X., *et al.*, The Effects of Jet Cavitation on the Growth of Microcystis Aeruginosa, *Journal of Environmental Science and Health, Part A, 41* (2006), 10, pp. 2345-2358
[8] Nor Saadah, Y., *et al.*, Physical and Chemical Effects of Acoustic Cavitation in Selected Ultrasonic Cleaning Applications, *Ultrasonics Sonochemistry, 29* (2016), Mar., pp. 568-576
[9] Filho, J. G. D., *et al.*, Bacterial Inactivation in Artificially and Naturally Contaminated Water Using a Cavitating Jet Apparatus, *Journal of Hydro-Environment Research, 9* (2015), 2, pp. 259-267
[10] Peng, G., Shimizu S., Progress in Numerical Simulation of Cavitating Water Jets, *Journal of Hydrodynamics, 25* (2013), 4, pp. 502-509
[11] Ahuja, V., *et al.*, Simulations of Cavitating Flows Using Hybrid Unstructured Meshes, *Journal of Fluid Engineering, ASME, 123* (2001), 2, pp. 331-340
[12] Barberon, T., Helluy, P., Finite Volume Simulation of Cavitating flows, *Computers &Fluids, 34* (2005). 7, pp. 832-858
[13] Barre, S., *et al.*, Experiments and Modelling of Cavitating Flows in Venturi: Attached Sheet Cavitation, *European Journal of Mechanics B-Fluids, 28* (2009), 3, pp. 444-464
[14] Guoyi, P., Seiji S., Progress in Numerical Simulation of Cavitating Water Jets, *Journal of Hydrodynamics, Ser. B, 25* (2013), 4, pp. 502-509
[15] Goncalves, E., Patella, R. F., Numerical Simulation of Cavitating Flows with Homogeneous Models, *Computers & Fluids, 38* (2009), 9, pp. 1682-1696
[16] Hutli, E., *et al.*, The Relation between the High Speed Submerged Cavitating Jet Behaviour and the Cavitation Erosion Process, *International Journal of Multiphase Flow, 83* (2016), July, pp. 27-38

[17] Hutli, E., *et al.*, Experimental Study on the Influence of Geometrical Parameters on the Cavitation Erosion Characteristics of High-Speed Submerged Jets, *Experimental Thermal and Fluid Science, 80* (2017), Jan., pp. 281-292
[18] Summers, D. A., Henry, R. L., Effect of Change in Energy and Momentum Levels on the Rock Removal Rate in Indiana Limestone, *Proceedings*, 1st International Symposium on Jet Cutting Technology, Coventry UK, 1972
[19] ***, http://citeseerx.ist.psu.edu/viewdoc/download?doi=10.1.1.40.531&rep=rep1&type=pdf
[20] Oh, T. M., Cho, G. C., Rock Cutting Depth Model Based on Kinetic Energy of Abrasive Waterjet, *Rock Mech Rock Eng, 49* (2016), 3, pp. 1059-1072
[21] Hutli, E., *et al*., An Experimental Investigation of Cavitating Jet Dynamic Power and Cavitation Intensity, *Proceedings*, ASME International Mechanical Engineering Congress and Exposition, IMECE2010-37488, Vancouver, British Columbia, Canada, 7 (2010), pp. 343-35
[22] Kalumuck, K. M., Chahine, G. L., The Use of Cavitating Jets To Oxidize Organic Compounds In Water, *Proceedings*, FJIDSM'98, ASME Fluids Engineering Division Summer Meeting, Washington, USA, 1998
[23] Kalumuck, K. M., *et al.*, Remediation and Disinfection of Water Using Jet Generated Cavitation, *Proceedings*, 5th International Symposium on Cavitation (CAV2003) Osaka, Japan 2003
[24] Hutli, E., Nedeljkovic M., Frequency in Shedding/Discharging Cavitation Clouds Determined by Visualization of a Submerged Cavitating Jet, *Journal of Fluid Engineering, ASME, 130* (2008), 2, ID 021304
[25] Zandi, A., *et al.*, Influence of Nozzle Geometry and Injection Conditions on the Cavitation Flow Inside a Diesel Injector, *International Journal of Automotive Engineering, 5* (2015), 1, pp. 939-954
[26] Momma, T., Lichtarowicz, A., A Study of Pressures and Erosion Produced by Collapsing Cavitation, *Wear, 186-187, Part 2* (1995), Aug., pp. 425-436
[27] ***, Mvt-Micro Technologies: Water Jet Cutting, http://www.mvt.ch
[28] Hutli, E. *et al.*, Appearance of High Submerged Cavitating Jet: The Cavitation Phenomenon and Sono-Luminescence, *Thermal Science, 17* (2013), 4, pp. 1151-1161
[29] Hutli, E. *et al.*, Influence of Hydrodynamic Conditions and Nozzle Geometry on Appearance of High Submerged Cavitating Jets, *Thermal Science, 17* (2013), 4, pp. 1139-1149
[30] Soyama, H., High-Speed Observation of a Cavitating Jet in Air, *Journal of Fluids Engineering, ASME, 127* (2005), 6, pp. 1095-1101
[31] Hiroyasu, H., Spray Breakup Mechanism from the Hole-Type Nozzle and its Applications, *Atomization Sprays, 10* (2000), 3-5, pp. 511-521
[32] Grinspan, A. S., Gnanamoorthy, R., Effect of Nozzle-Traveling Velocity on Oil Cavitation Jet Peening of Aluminum Alloy AA 6063-T6, *Journal of Engineering Materials and Technology, 129* (2007), 4, pp. 609-6014
[33] Tamaki, N, *et al.*, Enhancement of the Atomization of a Liquid Jet by Cavitation in a Nozzle Hole, *Atomization Sprays, 11* (2001), 2, pp. 125-137
[34] Tamaki, N, *et al.*, Effects of Cavitation and Internal Flow on Atomization of a Liquid Jet", *Atomization Sprays, 8* (1998), 2, pp. 179-197

Paper submitted: April 28, 2018
Paper revised: August 29, 2018
Paper accepted: September 3, 2018